RSC Advances

PAPER

View Article Online
View Journal | View Issue

Cite this: *RSC Adv.*, 2017, **7**, 31075

A novel AQDS–rGO composite to enhance the bioreduction of As(v)/Fe(iii) from the flooded arsenic-rich soil†

Zheng Chen,[abc] Jinfeng Zhang,[a] Kezeng Han,[a] Chaoying Yang,[a] Xiuli Jiang,[a] Dun Fu,[a] Qingbiao Li[a] and Yuanpeng Wang *[a]

Anthraquinone-2,6-disulphonate (AQDS) and reduced Graphene Oxide (rGO) were selected to prepare the AQDS–rGO composites for investigating the bioreduction performance of As(v)/Fe(iii) from the flooded arsenic-rich soil. The addition of AQDS–rGO composites coupled with acetate helped release more 849.87 ± 97.05 μg L^{-1} of As(iii) and 144.02 ± 10.02 mg L^{-1} of Fe(ii) from soil, compared to acetate control at 208.17 ± 35.97 μg L^{-1} of As(iii) and 85.75 ± 4.80 mg L^{-1} of Fe(ii). Meanwhile, the performance was also perceived to be better than the amendments with the mixture of gradient AQDS and acetate, as well as the incorporation of gradient AQDS, rGO and acetate (identified by the maximal levels of Fe(ii) and As(iii), less than 130.74 ± 22.01 mg L^{-1} and 675.15 ± 67.06 μg L^{-1}, respectively). Because metal-reducing or metal-oxidizing bacteria in the soil are susceptible to the soluble AQDS level, it would in turn influence the bioreduction performance of As(v)/Fe(iii). The mediated strategies of AQDS-composites positively correlated with the loaded contents of AQDS, electrical conductivity and increasing abundance of metal-reducing bacteria (*e.g.*, *Desulfitobacterium*, *Clostridium*, *Pseudomonas*, *Geobacter*, and *Anaeromyxobacter*) derived from the AQDS–rGO composites amendments, favor the bioreductive dissolution of As(v)/Fe(iii) from the soil. This insight will encourage the application of a promising tool as an alternative technology for remediating arsenic-polluted soil.

Received 12th May 2017
Accepted 12th June 2017

DOI: 10.1039/c7ra05393b

rsc.li/rsc-advances

1. Introduction

Soil arsenic (As) pollution has attracted increasing public attention in recent years, because of its strong threat and cancerogenic effect on humans and animals.[1] Elevated As levels occurring in groundwater has become a growing concern, resulting in the accumulation of As in agricultural crops through irrigation and runoff.[2,3] The main anthropogenic sources of As pollutants discharged into soil and water are mostly originated from metal mining and smelting, *e.g.*, the mining in realgar (As_4S_4) mines.[4] Especially, the weathering processes of abundant slag might seriously aggregate the regional As pollution in soil. Actually, the existence and enrichment of As in soil was closely related with iron (Fe) through coprecipitation and adsorption on the surface of iron oxides to form the arsenic–iron-minerals (*e.g.*, scorodite and lollingite).[5,6] Recent findings have demonstrated that the microbial activities derived from extracellular electron transfer (EET) would greatly promote the reductive dissolution of As(v)/Fe(iii) from the arsenic-bearing minerals in the flooded low oxygen or anoxic conditions, inevitably causing potential pollution to underground water.

Three approaches have been proposed for the process of EET: (1) through direct electron transfer; (2) long-ranged electron transfer through "conductive wires" formed by conductive materials (*e.g.*, pili and conductive materials); (3) mediated electron transfer by some quinoid- or flavin-based electron shuttle.[7] Although the process of EET has been extensively proven in many bioelectrochemistry fields—particularly in the microbial fuel cell systems and dissimilatory reduction of iron oxide by *Shewanella* or *Geobacter*[8,9]—the EET process within the bioreduction of As(v) was poorly explained. Our previous research has demonstrated that anthraquinone-2,6-disulphonate (AQDS) can facilitate the microorganism to transfer electrons extracellularly in the process of bioreduction of As(v) and Fe(iii) from soil.[10] Nevertheless, in practical application, AQDS was easily dispersed, usually causing the outcome of the increase in running costs and in secondary contamination.[11] Additionally, several specific adverse effects might result from the excess of AQDS.[12] Notably, the performance of EET derived from the coexistence of high level of AQDS and conductive material should

[a]*Department of Chemical and Biochemical Engineering, College of Chemistry and Chemical Engineering, Xiamen University, No. 422, Southern Siming Road, Xiamen 361005, China. E-mail: wypp@xmu.edu.cn*

[b]*Key Laboratory of Estuarine Ecological Security and Environmental Health, Tan Kah Kee College, Xiamen University, Zhangzhou, P. R. China*

[c]*Fujian Provincial Key Laboratory of Resource and Environment Monitoring & Sustainable Management and Utilization, Sanming, P. R. China*

† Electronic supplementary information (ESI) available. See DOI: 10.1039/c7ra05393b

not be underestimated, because it might elicit differential environmental influences. Moreover, a more plausible explanation seems to be that the performance of EET will be improved, armed with the presence of a powerful mediator that simultaneously assembles the features of electron shuttle and electrical conductivity. In spite of this, very limited researches reported that a powerful mediator owned such capacity of high-efficiency electron transport on promoting the bioreductive dissolution of As(v)/Fe(iii) from soil.

In order to balance the positive and negative impacts of AQDS on environmental application, various methods to immobilize AQDS were developed to prepare a powerful mediator. Graphene sheets with its high surface area, strong mechanical strength, and superior electrical conductivity could mediate the biotransformation of pollutants.[13,14] Some studies have indicated that reduced Graphene Oxide (rGO) could also mediate the biotransformation of pollutants. Thus rGO could not only be selected as carriers, but also prepared as AQDS–rGO composites to fulfill the specific functions. Besides, the functionalized composites of AQDS–rGO have also been tested as a special mediator for the reductive biotransformation of some organic pollutants under anaerobic consortium previously.[15] The evidence provided a broader future perspective upon applying functionalized composite to the bioreduction of metal contaminants. Thus, the exploration of the underlying mechanisms regarding how microbes mediate the reductive dissolution of As(v)/Fe(iii) from soil in the presence of the AQDS–rGO composites becomes an attractive area of study.

This study aims to evaluate the capability of AQDS–rGO composites to promote bioreduction of As(v)/Fe(iii) from the flooded arsenic-rich soil, sampled from an abandoned realgar mine. The performances and the mechanisms regarding bioreduction and mobilization of As(v)/Fe(iii) from soil were studied in detail. The results of this study would help to develop a promising technology for remediating the arsenic-polluted soil in future engineering management.

2. Materials and methods

2.1 Materials

The arsenic-polluted soils were sampled from an abandoned tailing realgar mine located in Shimen county, Hunan province, China. The soil in this area has been seriously polluted by arsenic.[16,17] The survey reported that the arsenic content (84.17–296.19 mg kg^{-1}) of soil within 3 villages near the mining sites far exceeded the safety value of soil environmental quality standards.[18] The soil was collected from the overburden layer of brushwood near an abandoned tailing mine, stored in sterile polyethylene bags, and then transported to the laboratory for further analyses. Some soils were air-dried, passed through a 2 mm sieve for the physicochemical analysis. The other non-dried samples were pre-purged with N_2, then strictly sealed to maintain the original environment for the indigenous microbes, and stored in a refrigerator at 4 °C until use. Table 1 describes the chemical compositions of elements contained in the sieved soil. The main minerals in soils were identified with the representative compounds of ferric arsenate [Fe(iii)As(v)O_4] through XRD analysis (Fig. S1†).

2.2 Preparation of AQDS–rGO composites and characterization

AQDS–rGO composites were prepared *via* a similar method proposed by Zhang *et al.* with a slight modification.[19] The preparation process could be described as following steps. The mixtures (0.05 g rGO powders and 100 mL AQDS solutions) were dispersed in 500 mL round-bottom flasks by water bath sonication for 2 h. AQDS solutions were set as 5.0, 10.0 and 25.0 mM, respectively. The aluminium foil was used to seal the flasks to avoid droplet splashing. The flasks were placed in a water bath at 80 °C and stirred for 24 h. Then, the reaction mixture was precipitated and cooled down to room temperature. 2 mL suspension was extracted to determine the corresponding remained AQDS content. Thereafter, the AQDS–rGO composites were separated, washed with deionized water, filtered through cellulose ester dialysis membranes (0.45 μm), and then vacuum-dried and weighed. The obtained AQDS–rGO composites that deposited by the least level of AQDS to the greatest level of AQDS were labeled as rGO-composite A, rGO-composite B, and rGO-composite C, respectively. According to the mass of obtained composites and the remained AQDS content of suspensions, the loaded capacities of AQDS in these 3 composites were approximately 4.06 $g_{(AQDS)}/g_{(rGO)}$ (rGO-composite A), 8.14 $g_{(AQDS)}/g_{(rGO)}$ (rGO-composite B), and 18.76 $g_{(AQDS)}/g_{(rGO)}$ (GO-composite C).

FTIR spectroscopy was employed to characterize quinone moieties on the surface of various prepared composites. The presence of C=O stretching of quinone moieties (1645 cm^{-1}) could be evidenced in FTIR spectra (Fig. S2†).[20] The increasing intensities of the peaks (1645 cm^{-1}) in FTIR spectra revealed that gradient contents of quinone moieties were loaded onto the surface of rGO-composites.

2.3 Assay design

Batch of anaerobic microcosm assays (15.00 g soil + 45.00 mL experimental solutions) was set up in triplicate in 105 mL serum bottles. The experimental substrates were amended with acetate coupled with various mediators, *i.e.*, rGO, AQDS, rGO–AQDS-incorporation and rGO-composites, respectively. The samples were bubbled under N_2/CO_2 (80 : 20) atmosphere for 0.5 h into

Table 1 Selected chemical compositions of elements in the sieved soil

Elements	C (%)	Organic-C (%)	N (%)	S (%)	Al (total) (g kg^{-1})	Mn (total) (g kg^{-1})	Fe (total) (g kg^{-1})	As (total) (mg kg^{-1})
Contents	0.75 − 0.86	0.37 − 0.42	0.22 − 0.25	0.76 − 0.85	90.28 ± 7.14	1.89 ± 0.34	36.13 ± 4.62	253.71 ± 10.12

liquid phase, then purged for another 0.5 h, and sealed under the same headspace. All samples were incubated at 30 °C in the dark. rGO used in this study was purchased from Chengdu Institute of Organic Chemistry of Chinese Academy of Sciences. The electrical conductivity of rGO was about 184 S cm^{-1}. The biotic amendments were followed as below (shown in Table S1†): soil amended with (i) acetate (the control assay), (ii) rGO coupled with acetate (denoted as rGO–acetate), (iii) AQDS coupled with acetate (denoted as AQDS–acetate), (iv) the mixtures of rGO, AQDS and acetate (denoted as AQDS–rGO-incorporation), and (v) the mixtures of rGO-composite and acetate (denoted as rGO-composite), respectively. The initial concentration of acetate solutions were set as 50.00 mM and rGO suspension was set as 40.00 mg L^{-1}. The AQDS solutions were set as 0.05, 0.10 and 1.00 mM, and rGO-composites (40.00 mg L^{-1}) were designated as rGO-composite A, rGO-composite B and rGO-composite C. Namely, the amendment ratio of rGO-composite and soil was set as 0.12 mg g^{-1}. Likewise, we simultaneously conducted another batch of abiotic assays, using sterile soil supplemented in turn with the same corresponding substrates. The aforementioned sterilization treatment was autoclaving at 120 °C for 20 min.

2.4 Analytical methods

2.4.1 Determination of Fe and As. At each sample point, certain volume suspensions from the microcosm culture assays were removed and filtered through a 0.45 μm filter for the determination of As(III), As(T) [total arsenic], Fe(II) and Fe(T) [total iron] in an anaerobic glove box. To determine Fe(T), a sample was reduced with 0.25 M hydroxylamine before the acid extraction.[21] The levels of Fe(T) and Fe(II) were quantified using the ferrozine assay.[22] Another filtered aqueous sample was analyzed for As(III) and As(T) levels using HG-AFS (AF-610B, China) and ICP-MS (Agilent 7700x, USA).

2.4.2 Determination of DOC and AQDS. The content of dissolved organic carbon (DOC) of suspension liquid were measured *via* a TOC analyzer (Shimadzu TOC-L CPH, Japan) after filtering supernatants with a Glass-Fiber Filter (Whatman, UK). The concentration of AQDS in liquid phase was measured at $\lambda = 328$ nm using a UV-visible spectrophotometer.[23] The filtered samples were diluted with bicarbonate buffer (60.00 mM) in an anaerobic glove box.

2.4.3 Measurement of the electrical conductivity of soil particles. Because of rGO-based mediators exhibiting superior electrical conductivity, it could be postulated that the electrical conductivity derived from soil particles might be increased in the presence of rGO-based mediators (included rGO and rGO-composites). Thus, armed with the presence of rGO-based mediators, the electrical conductivity derived from soil particles could be an important parameter to evaluate the role of electrical conductivity derived from the rGO-based mediators. In this study, the electrical conductivity of soil particles was evaluated using a specific-impedance-measuring device (Fig. S4†) designed by Dongping Zhan *et al.* from Engineering Research Center of Electrochemical Technology, Xiamen University, China. The detail measuring process was described in the ESI.†

2.5 DNA extraction, PCR amplification, sequencing and data analysis

Microbial DNA was extracted from 0.50 g soil samples (collected in an anaerobic glove box) using the Fast DNA Spin Kit for soil (MP Biomedical) according to manufacturer's protocols. The V4–V5 region of the bacteria 16S ribosomal RNA gene were amplified by PCR (95 °C for 3 min, followed by 27 cycles at 95 °C for 30 s, 55 °C for 30 s, and 72 °C for 45 s and a final extension at 72 °C for 10 min) using primers 338F ACTCCTACGGGAGGCAGCAG and 806R GGACTACHVGGGTWTCTAAT, where barcode is an eight-based sequence unique to each sample. PCR reactions were performed in triplicate 20.0 μL mixture containing 4.0 μL of 5 × FastPfu Buffer, 2.0 μL of 2.50 mM dNTPs, 0.80 μL of each primer (5.00 μM), 0.4 μL of FastPfu Polymerase, and 10.00 ng of template DNA.

Amplicons were extracted from 2% agarose gels and purified using the AxyPrep DNA Gel Extraction Kit (Axygen Biosciences, Union City, CA, U.S.) according to the manufacturer's instructions and quantified using QuantiFluor™-ST (Promega, U.S.). Purified amplicons were pooled in equimolar and paired-end sequenced (2 × 250) on an Illumina MiSeq platform according to the standard protocols. The raw reads were deposited into the NCBI Sequence Read Archive (SRA) database.

Raw fastq files were demultiplexed, quality-filtered using QIIME (version 1.17) with the following criteria: (i) The 300 bp reads were truncated at any site receiving an average quality score <20 over a 50 bp sliding window, discarding the truncated reads that were shorter than 50 bp; (ii) exact barcode matching, 2 nucleotide mismatch in primer matching, reads containing ambiguous characters were removed; (iii) only sequences that overlap longer than 10 bp were assembled according to their overlapping sequence. Reads which could not be assembled were discarded. Operational units (OTUs) were clustered with 97% similarity cutoff using UPARSE (version 7.1 http://www.drive5.com/uparse/) and chimeric sequences were identified and removed using UCHIME. The taxonomy of each 16S rRNA gene sequence was analyzed by RDP Classifier (http://www.rdp.cme.msu.edu/) against the silva (SSU115) 16S rRNA database using confidence threshold of 70%.[24]

2.6 Data statistics

The data were processed using SPSS 18.0 (SPSS Inc., Chicago, IL) and Origin 9.0 (Inc., OriginLab, Northampton, MA) softwares, and then expressed with the means ± standard deviation (SD). The treatment results were examined using analysis of variance (ANOVA). To analyze the statistical significance ($P < 0.05$) between pairs, the least significance difference (LSD) multiple range test was performed.

3. Results and discussion

3.1 Impact of AQDS on As(V) bioreduction

During the whole incubation period, very negligible levels of As(III) and As(T) were detected in all abiotic incubation assays (data not shown). Conversely, a favorable performance of reductive dissolution of As(V) from soil under biotic

amendments was observed, shown in Fig. 1a and b. Obviously, the As(III) levels derived from the amendments with rGO-composites were much higher than the As(III) levels from other batch experiments (Fig. 1c and d). A stronger enhancing bioreduction performance of As(V) was found in the amendment with rGO-composite that was loaded with higher contents of AQDS. Compared to the As(III) level derived from the control assay (208.17 ± 35.97 μg L^{-1}), approximately 1390.25 ± 69.01 μg L^{-1}, 1098.05 ± 58.02 μg L^{-1} and 849.87 ± 97.01 μg L^{-1} of the maximal As(III) levels were released with rGO-composite C, rGO-composite B and rGO-composite A, respectively. Additionally, the amendments with AQDS–rGO-incorporation were perceived to cause a differential effect on bioreduction performance of As(V). The results observed from the amendments with gradient AQDS–acetate and AQDS–rGO-incorporation implied that a more positive effect on bioreduction of As(V) resulted from 0.05 mM AQDS than 0.10 mM, but a significant inhibitory effect was indicated in 1.00 mM, regardless of rGO supplementation. Until the 47th day, approximately 2.5-, 1.9-, 2.1- and 1.5-fold of the maximal level of As(III) was detected in the amendment with 0.05 mM AQDS–rGO-incorporation, 0.10 mM AQDS–rGO-incorporation, 0.05 mM AQDS–acetate and 0.10 mM AQDS–acetate, respectively. Conversely, for the soil supplemented with redundant AQDS, the released levels of As(III) in the soil supplemented with 1.00 mM AQDS–rGO-incorporation and 1.00 mM AQDS–acetate were only less 0.8- and 0.5-fold increase compared to those in the soil supplemented with acetate alone on the 47th day.

3.2 Impact of AQDS on Fe(III) bioreduction

Likewise, nearly no soluble Fe(T) and Fe(II) levels were detected in all abiotic amendments (data not shown). The addition of rGO-composites mostly facilitated remarkable bioreduction of Fe(III) during the 47 days culture period (Fig. 2a and b), especially for the composites that were loaded with higher contents of AQDS. The maximal released levels of Fe(II) were approximately 144.02 ± 10.15 (rGO-composite A), 174.13 ± 9.05 (rGO-composite B) and 201.26 ± 11.02 mg L^{-1} (rGO-composite C) (Fig. 2c and d), respectively. Meanwhile, observations on the released levels of Fe(II) in amendments with AQDS–acetate and AQDS–rGO-incorporations indicated a differential impact. Compared to the assays amended with AQDS–acetate, the supplementation with rGO–acetate exhibited a slighter inhibitory effect on Fe(III) bioreduction. This could be attributed to the electrostatic attraction of cationic metal (iron ions) and rGO (with negative surface charge) (Table 2). However, the bioreduction performance of Fe(III) derived from the amendment with 0.05 mM AQDS–acetate was presented better than 0.10 mM AQDS–acetate, but unfavorable with 1.00 mM AQDS regardless of rGO supplementation. Compared to the control assays

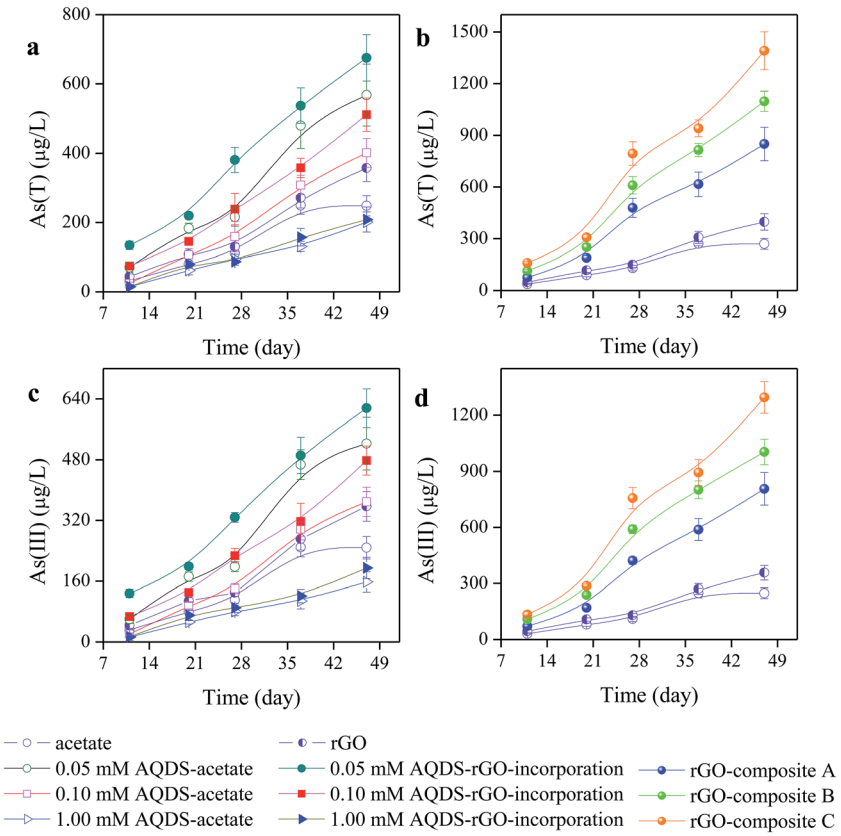

Fig. 1 Comparative soluble As(T) and As(III) levels derived from different amendments: (a) and (b) show the soluble As(T) levels derived from the amendments with gradient AQDS, gradient AQDS–rGO-incorporation and rGO-composites; while (c) and (d) show the soluble As(III) levels derived from the same corresponding conditions, respectively (the control assay was amended with acetate sodium alone).

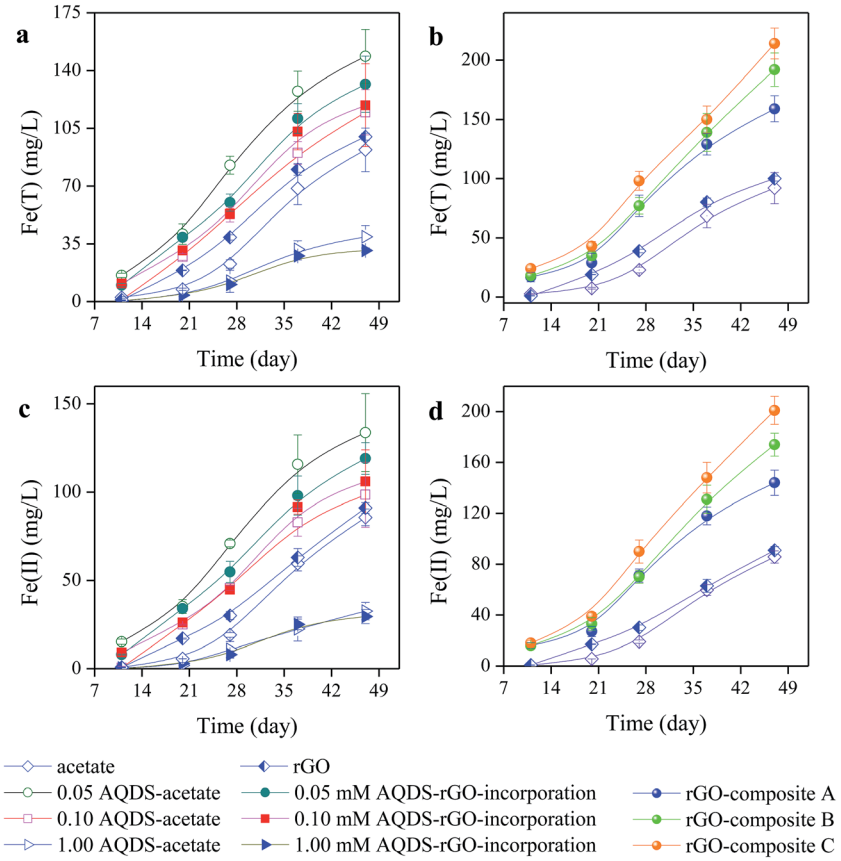

Fig. 2 Comparative the soluble Fe(T) and Fe(II) levels derived from different amendments: (a) and (b) show the soluble Fe(T) levels derived from the different rGO-based amendments; while (c) and (d) show the soluble Fe(II) levels derived from the same corresponding conditions.

Table 2 The impact of rGO to the sorption and speciation of Fe(II)/Fe(III) after 60 hour

Treatment	Initial Fe (mg L^{-1})	Fe(T) (mg L^{-1})	Fe(II) (mg L^{-1})	Fe(III) (mg L^{-1})	Adsorption fractions (%)
rGO + Fe(II)	50	12.01 ± 0.45	9.08 ± 0.77	2.93 ± 0.71	75.99
	75	17.97 ± 0.41	14.26 ± 3.38	3.72 ± 0.79	76.04
	100	28.22 ± 3.95	24.66 ± 0.51	3.56 ± 0.74	71.78
rGO + Fe(III)	50	5.18 ± 2.45	2.52 ± 1.67	2.66 ± 4.14	89.64
	75	10.86 ± 0.48	1.80 ± 0.03	9.05 ± 0.51	85.52
	100	16.85 ± 0.35	3.18 ± 0.57	13.67 ± 0.92	83.15

sampled on 47th day (85.75 ± 4.81 mg L^{-1}), approximately 1.6-, 1.3-, 1.4- and 1.2- fold of the maximal Fe(II) levels derived from the amendments with 0.05 mM AQDS–acetate, 0.10 mM AQDS–acetate, 0.05 mM AQDS–rGO-incorporation and 0.10 mM AQDS–rGO-incorporation were released, and approximately 0.4- and 0.3-fold increased Fe(II) levels were observed in the soil supplemented with 1.00 mM AQDS–acetate and 1.00 mM AQDS–rGO-incorporation.

On the whole, the results indicated an even stronger promoting effect on the bioreduction of As(V)/Fe(III) in the presence of a rGO-composite that was loaded with higher content of AQDS. Meanwhile, the coupling effect responding from rGO and AQDS could result in a partial boost on the reductive performance. Notably, however, the excessively redundant AQDS could suppress the bioreduction of As(V)/Fe(III) regardless of rGO supplementation. That is, the bioreductive performance of As(V)/Fe(III) was correlated with the dissolved AQDS level and the loaded contents of AQDS in composites.

Actually, the overall microbial conversion of pollutants was related to some specific effects (*e.g.*, substrate and microbial community change) driven by the varied mediators.[12,20,25] Thus, it is essential to explore the mechanisms derived from the mediators to demonstrate environmentally-influenced approaches, *e.g.*, the biotransformation of electron donors, the properties of mediator, and the shift of microbial community.

3.3 Dynamic change of DOC

The dynamic changes of DOC and AQDS were employed to evaluate the bioavailability of DOM (Fig. 3 and 4). Because AQDS

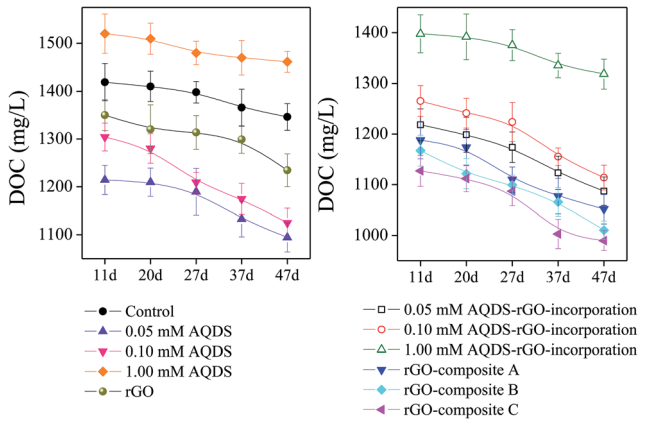

Fig. 3 The change of dissolved organic carbon (DOC) level.

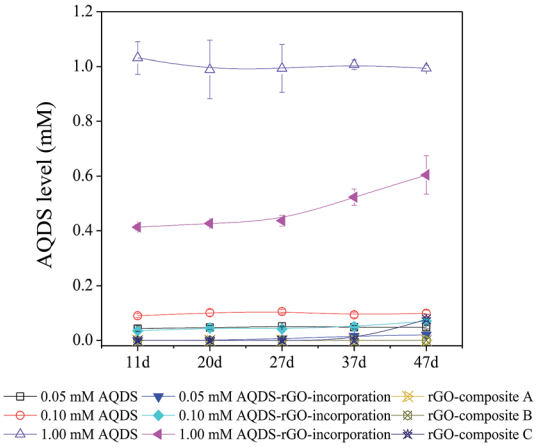

Fig. 4 The change of AQDS level in liquid phase.

serves as an electron shuttle, it confers the capacity to serve as an electron carrier in multiple redox reactions.[26] Correspondingly, AQDS levels appeared to be maintained at initial levels during the whole culture period in those assays in the absence of rGO (Fig. 4). A negligible level of AQDS (<0.01 mM) was observed in the amendments with rGO-composites and lower AQDS–rGO-incorporation (0.05 and 0.10 mM). The result was attributed to the sorption effect of rGO to AQDS. In the presence of higher AQDS (1.00 mM), some unadsorbed AQDS (0.42–0.61 mM) was still remained, and the effluent AQDS was gradually increasing in later culture period. Additionally, under the administration of exogenous matters (AQDS, rGO and rGO-composites), the consumption of electron donors was largely differently influenced (Fig. 3). A similar DOC change responsible for the corresponding mediator was revealed: starkly increased DOC bioavailability in rGO-composites amendments (27.78–31.05%), followed by the lower (0.05 and 0.10 mM) AQDS relevant amendments (21.74–24.08%), but less consumption in higher-level (1.00 mM) AQDS based assays (13.75–15.67%).

From these conflicting trends, it is possible to conclude that the influences of the mediator's selective preferences and level-dependent effect of AQDS govern the redox reactions. This suggestion was also in agreement with the bioreduction of As(v)/Fe(III). Notably, it should be pointed out that the process of extracellular electron transfer is more likely to be subjected to the fluctuation of functional microbial community and other specific mediation.[27] Thus, considering this possibility, the properties of AQDS–rGO-composites and the shift of the composition of microbial community deserve further attention.

3.4 Contributions of AQDS content and electrical conductivity derived from rGO-composite

Exactly, the preferentially influenced approach might be attributed to the properties of mediators in a limited magnitude. Because of the higher loaded content of AQDS and the enhancement of soil electrical conductivity, it might carry out a synergetic strategy to improve the electron transfer performance in the presence of rGO-composite. Actually, the observation on the rGO-composites amendments depicted that the reductive dissolution of Fe(III)/As(v) was positively correlated with the loaded contents of AQDS on the composites (Fig. 1 and 2). To make a further insightful clarification, the linear fitting curves (Fig. 5) offered a visual associations between the releasing levels of As(T)/As(III) and loaded contents of AQDS in rGO-composites. Through this immobilization method, AQDS was entrapped within the graphene sheets and kept with its redox mediating capacity. Additionally, using the rGO-composites to replace the AQDS–rGO-incorporation could also alleviate the inhibitory effect of redundant (1.00 mM) AQDS. In this study, rGO-composites promoted up to 1.6-fold increase on the bioreduction of As(v) and Fe(III), compared to the control that lacked supplementing AQDS.

Furthermore, the influenced mechanism was also correlated with the enhancement of electron transfer in the presence of rGO-based mediators. To probe the potential change of soil electrical conductivities acted by these mediators, the electrical conductivities of solid particles were evaluated according to the specific impedance-measuring-device (Fig. 6). As evidenced by the electrical conductivities of solid particles on 47th day, the electrical conductivities of soil particles derived from the amendments with rGO-composite A, rGO-composite B and rGO-composite C were approximately 1.9-, 2.0- and 2.2-fold greater than that of the control (198.05 $\pm$ 7.15 μs cm^{-1}), respectively. It

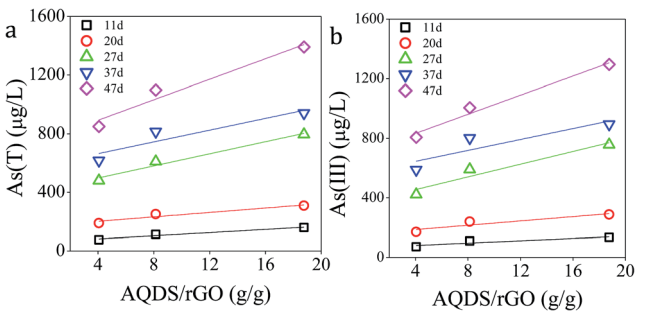

Fig. 5 The linear fitting curves between As(T)/As(III) and loading content of AQDS in composite: (a) As(T) *versus* AQDS/rGO and (b) As(III) *versus* AQDS/rGO.

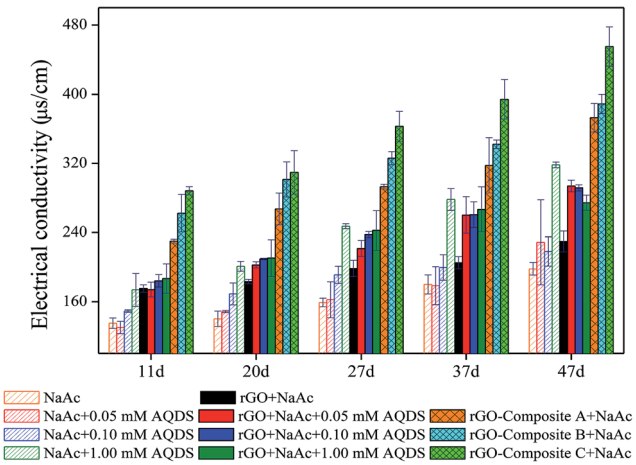

Fig. 6 Electrical conductivities of solid particles in the soil.

revealed that stronger electrical conductivity of soil particles was exhibited in the presence of rGO-composite, suggesting an advantage for electron transfer and redox reaction in the soil. In general, the variation trend of the electrical conductivities of solid particles was in agreement with the bioreduction of As(v)/Fe(iii): even more favorable reductive dissolution of As(v)/Fe(iii) and correspondingly higher electrical conductivity in soil could be confirmed. Because of the existence of localized π-electrons network associated with conductive graphene sheets regions, the bioreduction of As(v)/Fe(iii) might be partially radicalized.[28,29] Hence, this succession of synergistic effects was one available strategy for the electrons transfer on bioreduction of As(v)/Fe(iii).

3.5 Response to microbial community composition

In order to disclose the additional effects on the microbial community acted by these mediators, the relative abundances of the bacterial 16S rRNA gene at the phylum and genus level were examined to determine the affiliated composition of the microbial community (Fig. 7 and Table 3). The phyla diversity indicated the following: *Firmicutes* occupied the majority (65–77%), followed by *Proteobacteria* (15–20%), and *Actinobacteria* (3–7%) in all of amendments (Fig. 7a). Compared to the control amendment, we found a considerable discrepancy in genus abundance, including: *Bacillus* (33–39%), *Lactococcus* (20–24%), *Clostridium* (4–8%) and *Pseudomonas* (1–11%), where these mediators' treatment caused a selective influence—either promoting or reducing the abundance at certain magnitude (Fig. 7b).

Additionally, the abundance of selected oxidizing bacteria,[10,30] including *Alicyclobacillus*, *Burkholderia* and *Bradyrhizobium*, was collectively calculated to compare the mediator's contribution. Correspondingly, soil supplemented with 1.00 mM AQDS–acetate and 1.00 mM AQDS–rGO-incorporation exhibited increased abundance (9% and 14%) of metal-oxidizing bacteria (Table 3), which were significantly higher than the assigned abundances (2–3%) derived from other amendments. Besides, when summing the abundance of

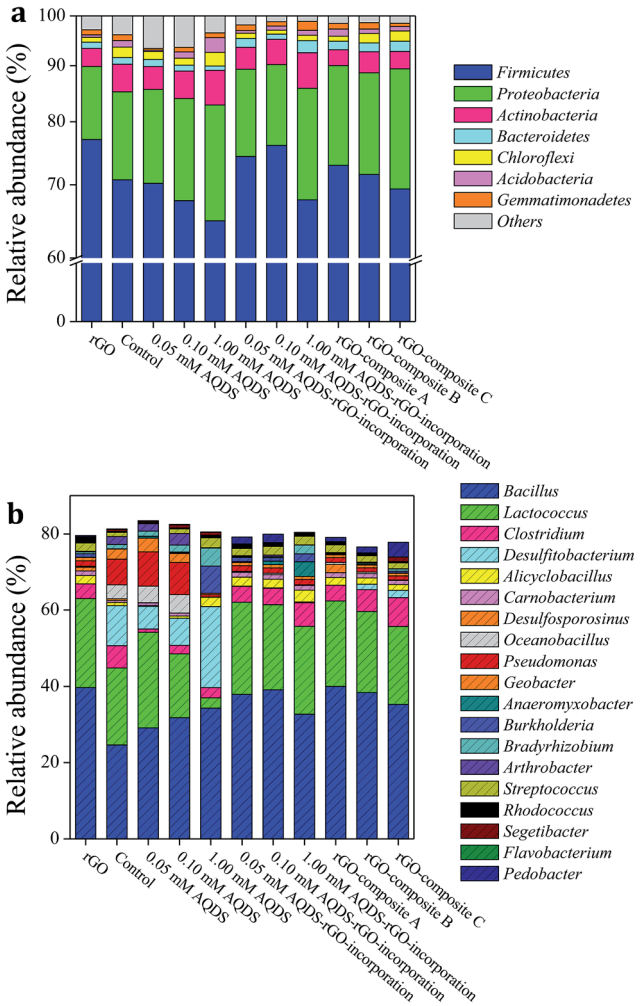

Fig. 7 Relative abundance of microbial community at phylum (a) and genus (b) level.

selected metal-reducing bacteria,[10,31] soil amended with lower (0.05 and 0.10 mM) AQDS–rGO-incorporations and rGO-composites exhibited increased abundance (8–17%) of *Desulfitobacterium*, *Clostridium*, *Pseudomonas*, *Geobacter* and *Anaeromyxobacter*, contrasting with the amendments with 1.00 mM AQDS–acetate (11%) and 1.00 mM AQDS–rGO-incorporation (10%). The result convincingly supported the involving mechanisms why these mediators' amendments selectively inhibited or promoted the reductive dissolution of As(v)/Fe(iii).

Fig. 8 shows the correlation between environmental factors and genera of microbial communities based on the regularized canonical correlation analysis (RCCA) by weighing the scores of both axes.[32] The scattered distribution of microbial community (Fig. 8a) was applied to distinguish the discrepancy of microbial communities based on the principal axis 1 scores (96%) on genus abundance. A close cluster location between rGO-composites amendments and lower AQDS–rGO-incorporation was presented, but was distant from the amendments with 1.00 mM AQDS–acetate and acetate alone. Furthermore, the RCCA indicated that the abundance associated with *Burkholderia* and *Bradyrhizobium* was positively correlated with

Table 3 The relative abundance (%) of selected metal-reducing or metal-oxidizing bacteria at genus level

	0.05 mM AQDS–rGO-incorporation	0.10 mM AQDS–rGO-incorporation	1.00 mM AQDS–rGO-incorporation	rGO-composite A	rGO-composite B	rGO-composite C
Selected metal-reducing bacteria						
Clostridium	4.19 ± 0.59	4.32 ± 0.81	6.18 ± 1.25	4.11 ± 0.59	5.74 ± 0.97	7.60 ± 0.88
Desulfitobacterium	0.04 ± 0.02	0.12 ± 0.01	0.23 ± 0.03	0.02 ± 0.03	1.41 ± 1.07	1.94 ± 1.62
Pseudomonas	1.48 ± 0.05	1.40 ± 0.07	1.42 ± 0.06	1.29 ± 0.19	1.13 ± 0.07	1.11 ± 0.06
Geobacter	0.86 ± 0.01	0.85 ± 0.02	0.81 ± 0.03	0.75 ± 0.11	0.75 ± 0.02	0.64 ± 0.02
Anaeromyxobacter	0.72 ± 0.05	0.94 ± 0.13	0.86 ± 0.49	2.14 ± 0.11	2.06 ± 0.54	2.47 ± 0.24
Selected metal-oxidizing bacteria						
Alicyclobacillus	2.36 ± 0.19	2.26 ± 0.15	3.10 ± 0.41	2.01 ± 0.52	1.66 ± 0.11	1.52 ± 0.10
Burkholderia	1.11 ± 0.61	0.93 ± 0.08	2.05 ± 0.15	0.18 ± 0.04	0.15 ± 0.01	0.48 ± 0.10
Bradyrhizobium	0.23 ± 0.05	0.31 ± 0.08	2.35 ± 0.28	0.23 ± 0.18	0.28 ± 0.11	0.63 ± 0.17

	Control	rGO	0.05 mM AQDS	0.10 mM AQDS	1.00 mM AQDS
Selected metal-reducing bacteria					
Clostridium	5.77 ± 1.09	3.87 ± 0.51	0.92 ± 0.21	2.18 ± 0.34	2.65 ± 0.34
Desulfitobacterium	10.54 ± 2.15	0.32 ± 0.08	5.93 ± 1.12	6.24 ± 1.12	21.25 ± 3.15
Pseudomonas	6.75 ± 1.38	1.43 ± 0.34	9.04 ± 1.84	8.40 ± 0.95	0.69 ± 0.09
Geobacter	2.65 ± 0.28	0.88 ± 0.15	3.61 ± 0.25	2.40 ± 0.10	0.38 ± 0.08
Anaeromyxobacter	0.09 ± 0.01	0.13 ± 0.08	0.47 ± 0.09	0.27 ± 0.03	0.09 ± 0.04
Selected metal-oxidizing bacteria					
Alicyclobacillus	0.84 ± 0.12	2.18 ± 0.35	0.24 ± 0.11	0.63 ± 0.02	2.48 ± 0.85
Burkholderia	0.11 ± 0.05	0.98 ± 0.18	0.09 ± 0.00	0.20 ± 0.01	7.15 ± 1.25
Bradyrhizobium	1.12 ± 0.09	0.58 ± 0.11	1.35 ± 0.09	1.79 ± 0.21	4.75 ± 0.81

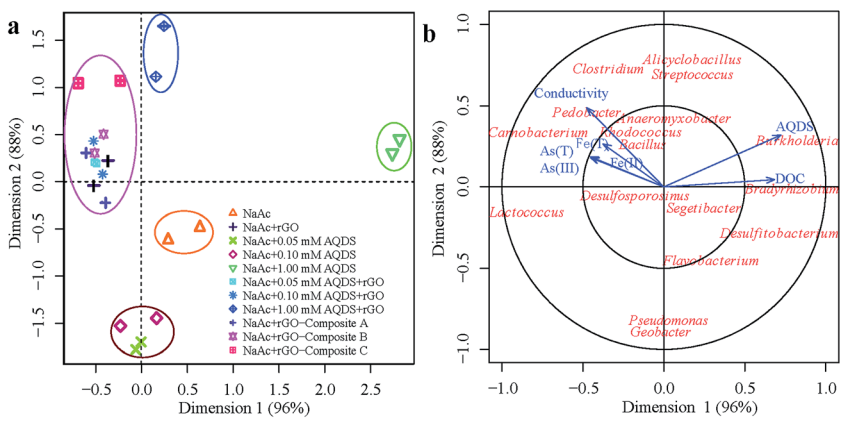

Fig. 8 Based on a regularized canonical correlation analysis (RCCA), the cluster plot of microbial community (a) and the two dimensional plot of microbial variables *versus* environmental factors (b) in rGO-based amendments.

DOC level and AQDS level (Fig. 8b). The Fe(T) level, Fe(II) level, As(T) level, As(III) level and electrical conductivity, however, demonstrated a positive correlation with *Bacillus*, *Rhodococcus* and *Pedobacter*. Collectively, the identification of these co-occurrence patterns suggested the special ecological contributions of varied mediators acting on the microbial community and metal-reducing process.

3.6 Implications for remediating soil arsenic pollution

The involving mechanism of rGO-composites was suggested in Fig. 9. A synergetic strategy was carried out to promote the *in situ* reductive dissolution of As(V)/Fe(III) from arsenic-rich soil. (1) The shuttling compounds—AQDS loaded in the composites is one important prerequisite on the redox reaction. (2) The electrical conductivity derived from the rGO-composites improves the performance of EET. (3) The addition of rGO-composites shifts the composition of microbial community and boosts the enrichments of some metal-reducing bacteria, further enabling the bioreduction of As(V)/Fe(III). Moreover, previous investigations demonstrated that the conjugated π–π structure of graphene sheets and AQDS activated the electrically catalytic regions of electron hoping, expanding the attached

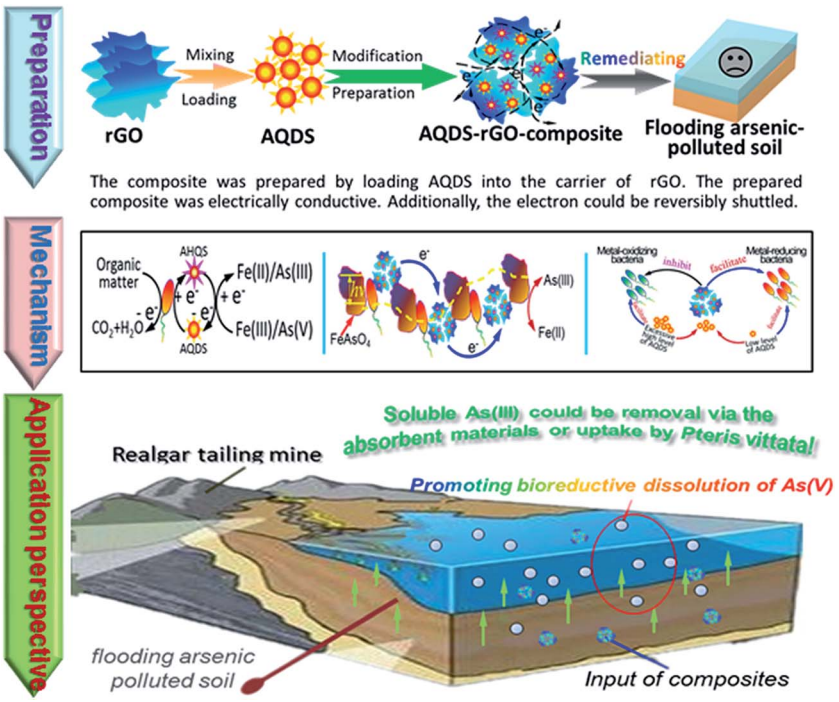

Fig. 9 The mechanism of AQDS–rGO-composite affecting bioreductive dissolution of As(v)/Fe(iii) from flooded arsenic-polluted soil.

spaces between electrons, microbe and metal-oxides, accelerating the electron transfer.[33,34]

EET has been gaining wide interest in relation to biotransformation of pollutants and the microbial bioremediation for the metal pollutants.[9,35] A large numbers of researches have been focused on EET process derived from AQDS.[10,12,26] Very limited research has reported a powerful mediator that simultaneously assembles the features of electron shuttle and electrical conductivity. In this study, AQDS–rGO-composite, with the support of rGO and AQDS, rapidly channeled the electrons transferring from electron donors (*e.g.* acetate and soil organic) to electron acceptors (As(v) and Fe(iii)), promoting the bioreduction performance of As(v)/Fe(iii). A special consortium within "microbe-mediator-arsenic-bearing minerals" was disclosed to mediate the mobilization of As and Fe from flooded soil, arousing our attention to exploit feasible bioremediation for arsenic-polluted soil.

For the disposal of arsenic-polluted soil, the previous treatment was to deposit arsenic by incorporating ferrite as arsenic–iron-minerals.[36] This method seems to be effective. However, the presence of these arsenic-bearing minerals might potentially lead in the pollution of groundwater.[37,38] Especially in the flooded anoxic condition, arsenic depositing methods might be just a "temporary remedy of relief" but without dealing with the soil arsenic contaminants eventually. Thus, to decrease the background content of As in soil was an important prerequisite to effectively remedy the arsenic-polluted soil. It was reported that some hyperaccumulators and functional absorbent materials, *e.g.*, *Pteris vittata* and layered double hydroxides, were capable to adsorb the soluble As ions.[39,40] The concept of promoting the conversion of insoluble arsenic-bearing minerals from polluted soil into the soluble As ions, which are subsequently removal *via* absorbent materials or uptake by *Pteris vittata* could be proposed as a feasible remediation approach for the removal of As from contaminated soil sites. Nevertheless, applying available chemical and microbial remediation on the real arsenic-polluted soil has just acquired surprisingly little systematic investigation to date. In this study, AQDS–rGO composites displayed better catalytic performance for As(v) bioreduction compared to soluble AQDS, indicating that AQDS–rGO composites acted as a solid-phase redox mediator to accelerate the As(v) bioreduction. Hence, the findings from this study are both profound biogeochemical and applied engineering implications for the future application on *in situ* bioremediating soil metal-pollution.

Moreover, insight from our study might also encourage the successful application of quinones for bioremediation in the future. In view of representative quinone-containing AQDS materials, AQDS could potentially be applicable as a mediator in flooded soil bioremediation and underground water treatment.[41] Because quinones are significantly abundant in humus and are considered as inexpensively available organic matter, they should be considered as potential sources for redox materials.[26] Favorable catalytic activity/stability and acceleration of the bioreductive transformation of pollutants are crucial parameters for this process. Thus, considering the variety of bioremediation needs that might require the application of AQDS, further optimization of AQDS-composite materials to fulfill specific functions is required, as is the balancing of their positive and negative impact for environmental safety.

4. Conclusions

It was observed that the supplementation with AQDS in gradient levels exhibited a differential performance of electron transfer, regardless of the presence of rGO. A more favorable effect on the bioreduction of As(v)/Fe(iii) was perceived in lower (0.05 mM) AQDS-based amendments than in low (0.10 mM) AQDS-based amendments, whereas an inhibitory performance resulted from higher AQDS (1.00 mM)-based amendments. The supplementation with rGO-composites, however, greatly improved the bioreduction performance of As(v)/Fe(iii), particularly the composite that was loaded with higher content of AQDS. Relevant mediating strategies were linked to the loaded content of AQDS and the electrical conductivity derived from the rGO-composites, as well as the increasing abundances of some metal-reducing bacteria under the application of rGO-composites. Collectively, the findings in our study might contribute to developing a promising alternative technology for remediating the arsenic-polluted soil in the future.

Acknowledgements

This work was supported by the National Basic Research Program of China (2013CB733505), the National Natural Science Foundation of China (41571449, 41271260, 41276101 and 41301346) and Fundamental Research Funds for the Central Universities of China (20720160083).

References

1 A. A. Meharg and M. Rahman, *Environ. Sci. Technol.*, 2003, **37**, 229–234.
2 H. Y. Yu, X. Ding, F. Li, X. Wang, S. Zhang, J. Yi, C. Liu, X. Xu and Q. Wang, *Environ. Pollut.*, 2016, **215**, 258–265.
3 A. A. Meharg, *Trends Plant Sci.*, 2004, **9**, 415–417.
4 Y. Wu, X.-y. Zhou, M. Lei, J. Yang, J. Ma, P.-w. Qiao and T.-b. Chen, *Appl. Geochem.*, 2017, **77**, 44–51.
5 D. Paktunc and K. Bruggeman, *Appl. Geochem.*, 2010, **25**, 674–683.
6 M. Filippi, *Sci. Total Environ.*, 2004, **322**, 271–282.
7 O. Choi and B. I. Sang, *Biotechnol. Biofuels*, 2016, **9**, 1–14.
8 M. Shimizu, J. Zhou, C. Schroder, M. Obst, A. Kappler and T. Borch, *Environ. Sci. Technol.*, 2013, **47**, 13375–13384.
9 R. Kumar, L. Singh and A. W. Zularisam, *Renewable Sustainable Energy Rev.*, 2016, **56**, 1322–1336.
10 Z. Chen, Y. Wang, X. Jiang, D. Fu, D. Xia, H. Wang, G. Dong and Q. Li, *Sci. Total Environ.*, 2017, **574**, 1684–1694.
11 W. Jing, L. Lihua, Z. Jiti, L. Hong, L. Guangfei, J. Ruofei and Y. Fenglin, *J. Hazard. Mater.*, 2009, **168**, 1098–1104.
12 J. L. Xu, L. Zhuang, G. Q. Yang, Y. Yuan and S. G. Zhou, *Microb. Ecol.*, 2013, **66**, 950–960.
13 X. Yin, S. Qiao, J. T. Zhou and X. Tang, *Chem. Eng. J.*, 2016, **283**, 160–166.
14 Y. Yuan, S. G. Zhou, B. Zhao, L. Zhuang and Y. Q. Wang, *Bioresour. Technol.*, 2012, **116**, 453–458.
15 H. Lu, H. K. Zhang, J. Wang, J. T. Zhou and Y. Zhou, *RSC Adv.*, 2014, **4**, 47297–47303.
16 Z. C. Huang, T. B. Chen, M. Lei, Y. R. Liu and T. D. Hu, *Environ. Sci. Technol.*, 2008, **42**, 5106–5111.
17 X. Lu and X. Zhang, *Environ. Geochem. Health*, 2005, **27**, 313–320.
18 Y.-M. Zhu, C.-Y. Wei and L.-S. Yang, *Acta Ecol. Sin.*, 2010, **30**, 178–183.
19 H. K. Zhang, H. Lu, J. Wang, J. T. Zhou and M. Sui, *Environ. Sci. Technol.*, 2014, **48**, 12876–12885.
20 C. F. Zhang and A. Katayama, *Environ. Sci. Technol.*, 2012, **46**, 6575–6583.
21 S. Kato, K. Hashimoto and K. Watanabe, *Proc. Natl. Acad. Sci. U. S. A.*, 2012, **109**, 10042–10046.
22 E. Viollier, P. W. Inglett, K. Hunter, A. N. Roychoudhury and P. Van Cappellen, *Appl. Geochem.*, 2000, **15**, 785–790.
23 L. H. Alvarez, M. A. Perez-Cruz, J. R. Rangel-Mendez and F. J. Cervantes, *J. Hazard. Mater.*, 2010, **184**, 268–272.
24 K. R. Amato, C. J. Yeoman, A. Kent, N. Righini, F. Carbonero, A. Estrada, H. R. Gaskins, R. M. Stumpf, S. Yildirim, M. Torralba, M. Gillis, B. A. Wilson, K. E. Nelson, B. A. White and S. R. Leigh, *ISME J.*, 2013, **7**, 1344–1353.
25 J. Rau, H. J. Knackmuss and A. Stolz, *Environ. Sci. Technol.*, 2002, **36**, 1497–1504.
26 F. R. Van der Zee and F. J. Cervantes, *Biotechnol. Adv.*, 2009, **27**, 256–277.
27 Y. X. Zhao, J. R. Swierk, J. D. Megiatto, B. Sherman, W. J. Youngblood, D. D. Qin, D. M. Lentz, A. L. Moore, T. A. Moore, D. Gust and T. E. Mallouk, *Proc. Natl. Acad. Sci. U. S. A.*, 2012, **109**, 15612–15616.
28 H. Fu and D. Zhu, *Environ. Sci. Technol.*, 2013, **47**, 4204–4210.
29 X. Zhang, Z. Sui, B. Xu, S. Yue, Y. Luo, W. Zhan and B. Liu, *J. Mater. Chem.*, 2011, **21**, 6494–6497.
30 M. Sultana, S. Vogler, K. Zargar, A. C. Schmidt, C. Saltikov, J. Seifert and M. Schlomann, *Arch. Microbiol.*, 2012, **194**, 623–635.
31 E. S. Shelobolina, C. G. Vanpraagh and D. R. Lovley, *Geomicrobiol. J.*, 2003, **20**, 143–156.
32 I. Gonzalez, S. Dejean, P. G. P. Martin and A. Baccini, *J. Stat. Software*, 2008, **23**, 1–14.
33 Y. Yuan, J. Ahmed and S. Kim, *J. Power Sources*, 2011, **196**, 1103–1106.
34 T. Sizun, T. Patois, M. Bouvet and B. Lakard, *J. Mater. Chem.*, 2012, **22**, 25246–25253.
35 D. R. Lovley, *Curr. Opin. Biotechnol.*, 2006, **17**, 327–332.
36 E. Krause and V. A. Ettel, *Hydrometallurgy*, 1989, **22**, 311–337.
37 M. A. Armienta, G. Villaseñor, R. Rodriguez, L. K. Ongley and H. Mango, *Environ. Geol.*, 2001, **40**, 571–581.
38 P. Drahota and M. Filippi, *Environ. Int.*, 2009, **35**, 1243–1255.
39 T. B. Chen, C. Y. Wei, Z. C. Huang, Q. F. Huang, Q. G. Lu and Z. L. Fan, *Chin. Sci. Bull.*, 2002, **47**, 902–905.
40 L. Shen, X. Jiang, Z. Chen, D. Fu, Q. Li, T. Ouyang and Y. Wang, *Chemosphere*, 2017, **176**, 57–66.
41 I. V. Perminova, K. Hatfield and N. Hertkorn, *Use of humic substances to remediate polluted environments: from theory to practice*, Springer, Netherlands, 2005.

